Harnessing the host immune system constitutes a promising cancer therapeutic because of its potential to specifically target tumor cells although limiting harm to normal tissue. Enthusiasm has been fueled by recent clinical success, particularly with antibodies that block immune inhibitory pathways, specifically CTLA-4 and the axis between programmed cell death protein 1 (PD-1) and its ligand 1 (PD-L1) (*1*, *2*). Clinical responses to these immunotherapies are more frequent in patients who show evidence of an endogenous T cell response ongoing in the tumor microenvironment before therapy (*3*–*6*). However, the mechanisms that govern the presence or absence of this phenotype are not well understood. Theoretical sources of interpatient heterogeneity include host germline genetic differences, variability in patterns of somatic alterations in tumor cells, and environmental differences.

The gut microbiota plays an important role in shaping systemic immune responses (*7*–*9*). In the cancer context, a role for intestinal microbiota in mediating immune activation in response to chemotherapeutic agents has been demonstrated (*10*, *11*). However, it is not known whether commensal microbiota influence spontaneous immune responses against tumors and thereby affect the therapeutic activity of immunotherapeutic interventions, such as anti–PD-1/PD-L1 monoclonal antibodies (mAbs).

To address this question, we compared subcutaneous B16.SIY melanoma growth in genetically similar C57BL/6 mice derived from two different mouse facilities, Jackson Laboratory (JAX) and Taconic Farms (TAC), which have been shown to differ in their commensal microbes (*12*). We found that JAX and TAC mice exhibited significant differences in B16.SIY melanoma growth rate, with tumors growing more aggressively in TAC mice (Fig. 1A). This difference was immune-mediated: Tumor-specific T cell responses (Fig. 1, B and C) and intratumoral $CD8^+$ T cell accumulation (Fig. 1D) were significantly higher in JAX than in TAC mice. To begin to address whether this difference could be mediated by commensal microbiota, we cohoused JAX and TAC mice before tumor implantation. We found that cohousing ablated the differences in tumor growth (Fig. 1E) and immune responses (Fig. 1, F to H) between the two mouse populations, which suggested an environmental influence. Cohoused TAC and JAX mice appeared to acquire the JAX phenotype, which suggested that JAX mice may be colonized by commensal microbes that dominantly facilitate antitumor immunity.

To directly test the role of commensal bacteria in regulating antitumor immunity, we transferred JAX or TAC fecal suspensions into TAC and JAX recipients by oral gavage before tumor implantation (fig. S1A). We found that prophylactic transfer of JAX fecal material, but not saline or TAC fecal material, into TAC recipients was sufficient to delay tumor growth (Fig. 2A) and to enhance induction and infiltration of tumor-specific $CD8^+$ T cells (Fig. 2, B and C, and fig. S1B), which supported a microbe-derived effect. Reciprocal transfer of TAC fecal material into JAX recipients had a minimal effect on tumor growth rate and antitumor T cell responses (Fig. 2, A to C, and fig. S1B), consistent with the JAX-dominant effects observed upon cohousing.

To test whether manipulation of the microbial community could be effective as a therapy, we administered JAX fecal material alone or in combination with antibodies targeting PD-L1 (αPD-L1) to TAC mice bearing established tumors. Transfer of JAX fecal material alone resulted in significantly slower tumor growth (Fig. 2D), accompanied by increased tumor-specific T cell responses (Fig. 2E) and infiltration of antigen-specific T cells into the tumor (Fig. 2F), to the same degree as treatment with systemic αPD-L1 mAb. Combination treatment with both JAX fecal transfer and αPD-L1 mAb improved tumor control (Fig. 2D) and circulating tumor antigen–specific T cell responses (Fig. 2E), although there was little additive effect on accumulation of activated T cells within the tumor microenvironment (Fig. 2F). Consistent with these results, αPD-L1 therapy alone was significantly more efficacious in JAX mice compared with TAC mice (Fig. 2G), which paralleled improved antitumor T cell responses (fig. S1C). These data indicate that the commensal microbial composition can influence spontaneous antitumor immunity, as well as a response to immunotherapy with αPD-L1 mAb.

To identify specific bacteria associated with improved antitumor immune responses, we monitored the fecal bacterial content over time of mice that were subjected to administration of fecal permutations, using the 16*S* ribosomal RNA (rRNA) miSeq Illumina platform. Principal coordinate analysis revealed that fecal samples analyzed from TAC mice that received JAX fecal material gradually separated from samples obtained from sham- and TAC feces–inoculated TAC mice over time ($P = 0.001$ and $P = 0.003$, respectively, ANOSIM multivariate data analysis) and became similar

[1]Department of Pathology, University of Chicago, Chicago, IL 60637, USA. [2]Department of Medicine, University of Chicago, Chicago, IL 60637, USA. [3]Section of Genetic Medicine, University of Chicago, Chicago, IL 60637, USA.
*These authors contributed equally to this work. †Corresponding author. E-mail: tgajewsk@medicine.bsd.uchicago.edu

to samples obtained from sham- and JAX feces–inoculated JAX mice (Fig. 3A). In contrast, TAC-inoculated TAC mice did not change in community diversity relative to sham-inoculated TAC mice (P = 0.4, ANOSIM). Reciprocal transfer of TAC fecal material into JAX hosts resulted in a statistically significant change in community diversity (P = 0.003, ANOSIM), yet the distance of the microbial shift was smaller (Fig. 3A).

Comparative analysis showed that 257 taxa were of significantly different relative abundance in JAX mice relative to TAC mice [false discovery rate (FDR) < 0.05, nonparametric t test] (Fig. 3B and table S1). Members belonging to several of these groups were similarly altered in JAX-fed TAC mice relative to sham- or TAC-inoculated TAC mice (Fig. 3C and tables S1 and S2). To further identify functionally relevant bacterial taxa, we asked which genus-level taxa were significantly associated with accumulation of activated antigen-specific T cells within the tumor microenvironment across all permutations (Fig. 2C). The only significant association was *Bifidobacterium* (P = 5.7×10^{-5}, FDR = 0.0019, univariate regression) (table S3), which showed a positive association with antitumor T cell responses and increased in relative abundance over 400-fold in JAX-fed TAC mice (Fig. 3C). Stimulatory interactions between bifidobacteria and the host immune system, including those associated with interferon-γ (IFN-γ), have been described previously (*13*–*16*). We thus hypothesized that members of this genus could represent a major component of the beneficial antitumor immune effects observed in JAX mice.

At the sequence level, *Bifidobacterium* operational taxonomic unit OTU_681370 showed the largest increase in relative abundance in JAX-fed TAC mice (table S1) and the strongest association with antitumor T cell responses across all permutations (Fig. 3D and table S3). We further identified this bacterium as most similar to *B. breve*, *B. longum*, and *B. adolescentis* (99% identity). To test whether *Bifidobacterium* spp. may be sufficient to augment protective immunity against tumors, we obtained a commercially available cocktail of *Bifidobacterium* species, which included *B. breve* and *B. longum* and administered this by oral gavage, alone or in combination with αPD-L1, to TAC recipients bearing established tumors. Analysis of fecal bacterial content revealed that the most significant change in response to *Bifidobacterium* inoculation occurred in the *Bifidobacterium* genus (P = 0.0009, FDR = 0.015, nonparametric t test), with a 120-fold increase in OTU_681370 (fig. S2A and table S4), which suggested that the commercial inoculum contained bacteria that were at least 97% identical to the taxon identified in JAX and JAX-fed TAC mice. An increase in *Bifidobacterium* could also be detected by quantitative polymerase chain reaction (PCR) (fig. S2B).

Bifidobacterium-treated mice displayed significantly improved tumor control in comparison with their non-*Bifidobacterium* treated counterparts (Fig. 3E), which was accompanied by robust induction of tumor-specific T cells in the periphery (Fig. 3F) and increased accumulation of antigen-specific $CD8^+$ T cells within the tumor

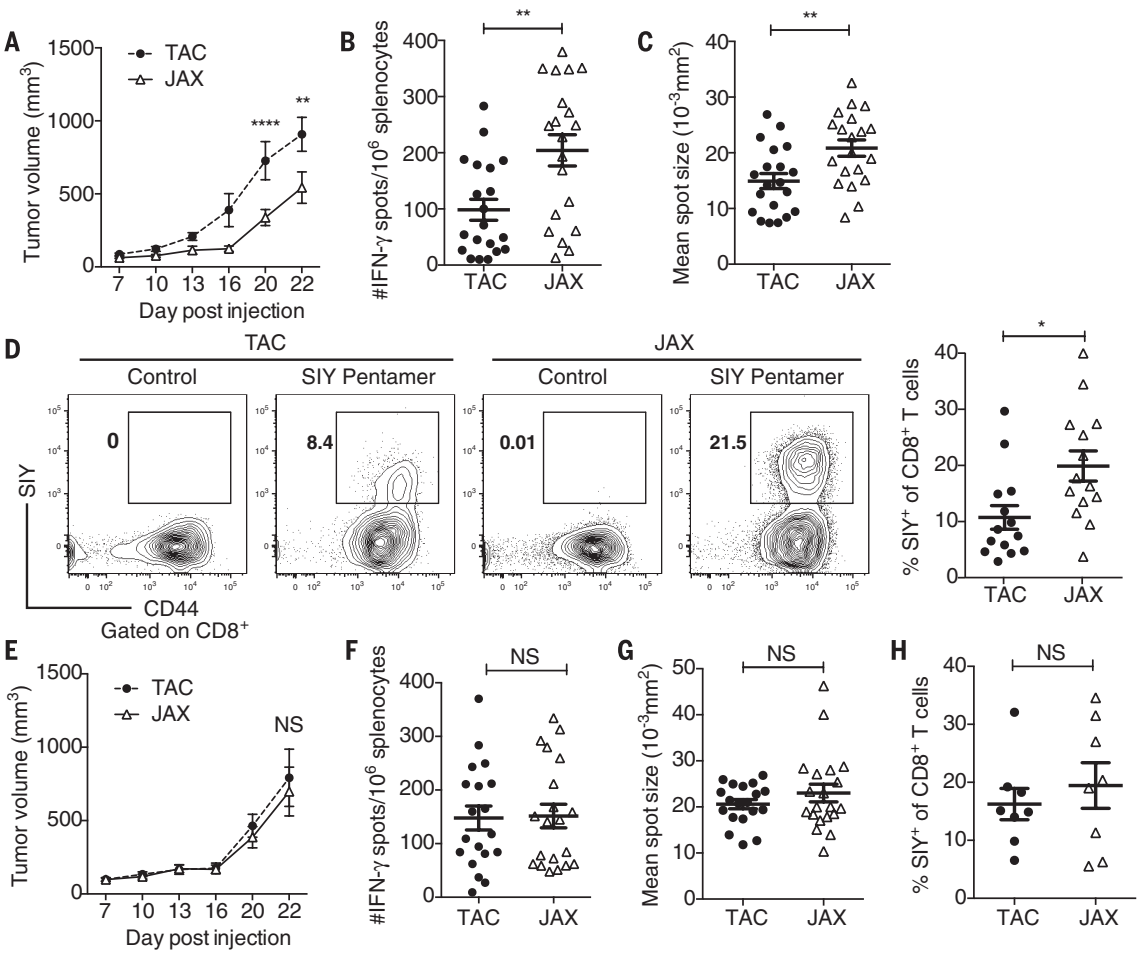

Fig. 1. Differences in melanoma outgrowth and tumor-specific immune responses between C57BL/6 JAX and TAC mice are eliminated when mice are cohoused. (**A**) B16.SIY tumor growth kinetics in newly arrived JAX and TAC mice. (**B**) IFN-γ enzyme-linked immunospot assay (ELISPOT) in tumor-bearing JAX and TAC mice 7 days after tumor inoculation. (**C**) Mean size of IFN-γ spots (10^{-3} mm^2). (**D**) Percentage of SIY^+ T cells of total $CD8^+$ T cells within the tumor of JAX and TAC mice as determined by flow cytometry 21 days after tumor inoculation. Representative plots (left), quantification (right). (**E**) B16.SIY tumor growth kinetics in JAX and TAC mice cohoused for 3 weeks before tumor inoculation. (**F**) Number of IFN-γ spots/10^6 splenocytes in tumor-bearing JAX and TAC mice cohoused for 3 weeks before tumor inoculation. (**G**) Mean size of IFN-γ spots (10^{-3} mm^2). (**H**) Percentage of SIY^+ T cells of total $CD8^+$ T cells within the tumor of JAX and TAC mice cohoused for 3 weeks before tumor inoculation. Means ± SEM combined from six independent experiments, analyzed by two-way analysis of variance (ANOVA) with Sidak's correction for multiple comparisons (A) and (E), or individual mice with means ± SEM combined from four (B), (C), (F), (G) or three (D) and (H) independent experiments, analyzed by Student's t test; five mice per group per experiment; *P < 0.005, **P < 0.01; NS, not significant.

(Fig. 3G and fig. S2C). These effects lasted several weeks (fig. S2, D and E).

The therapeutic effect of *Bifidobacterium* feeding was abrogated in CD8-depleted mice (fig. S3A), which indicated that the mechanism was not direct but rather through host antitumor T cell responses. Heat inactivation of the bacteria before oral administration also abrogated the therapeutic effect on tumor growth and reduced tumor-specific T cell responses to baseline (fig. S3, B to D), which suggested that the antitumor effect requires live bacteria. As an alternative strategy, we tested the therapeutic effect of *B. breve* and *B. longum* strains obtained from the American Type Culture Collection, which also showed significantly improved tumor control (fig. S4A). Administration of *Bifidobacterium* to TAC mice inoculated with B16 parental tumor cells or MB49 bladder cancer cells also resulted in delayed tumor outgrowth (fig. S4, B and C, respectively). Oral administration of *Lactobacillus murinus* to TAC mice, which was not among the overrepresented taxa in JAX-fed mice, had no effect on tumor growth (fig. S4D) or on tumor-specific T cell responses (fig. S4E), which suggested that modulation of antitumor immunity depends on the specific bacteria administered. Collectively, these data point to *Bifidobacterium* as a positive regulator of antitumor immunity in vivo.

Upon inoculation with *Bifidobacterium*, a small set of species were altered in parallel with *Bifidobacterium* (ANOSIM, $P = 0.003$) (fig. S5A and table S4), however, for the most part, they did not resemble the changes observed with JAX feces administration. Although we observed reductions (~2- to 10-fold) in members of the order Clostridiales, as well as in butyrate-producing species, upon *Bifidobacterium* inoculation, which could point to an inhibitory effect on the regulatory T cell compartment (*17*–*19*), we did not observe any difference in the frequency of $CD4^+$ $Foxp3^+$ T cells in tumors isolated from JAX and TAC mice (fig. S5B). Thus, although we cannot definitively rule out an indirect effect, it is unlikely that *Bifidobacterium* is acting primarily through modulation of the abundance of other bacteria.

We next assessed whether translocation of *Bifidobacterium* was occurring into the mesenteric lymph nodes, spleen, or tumor; however, no *Bifidobacterium* was detected in any of the organs

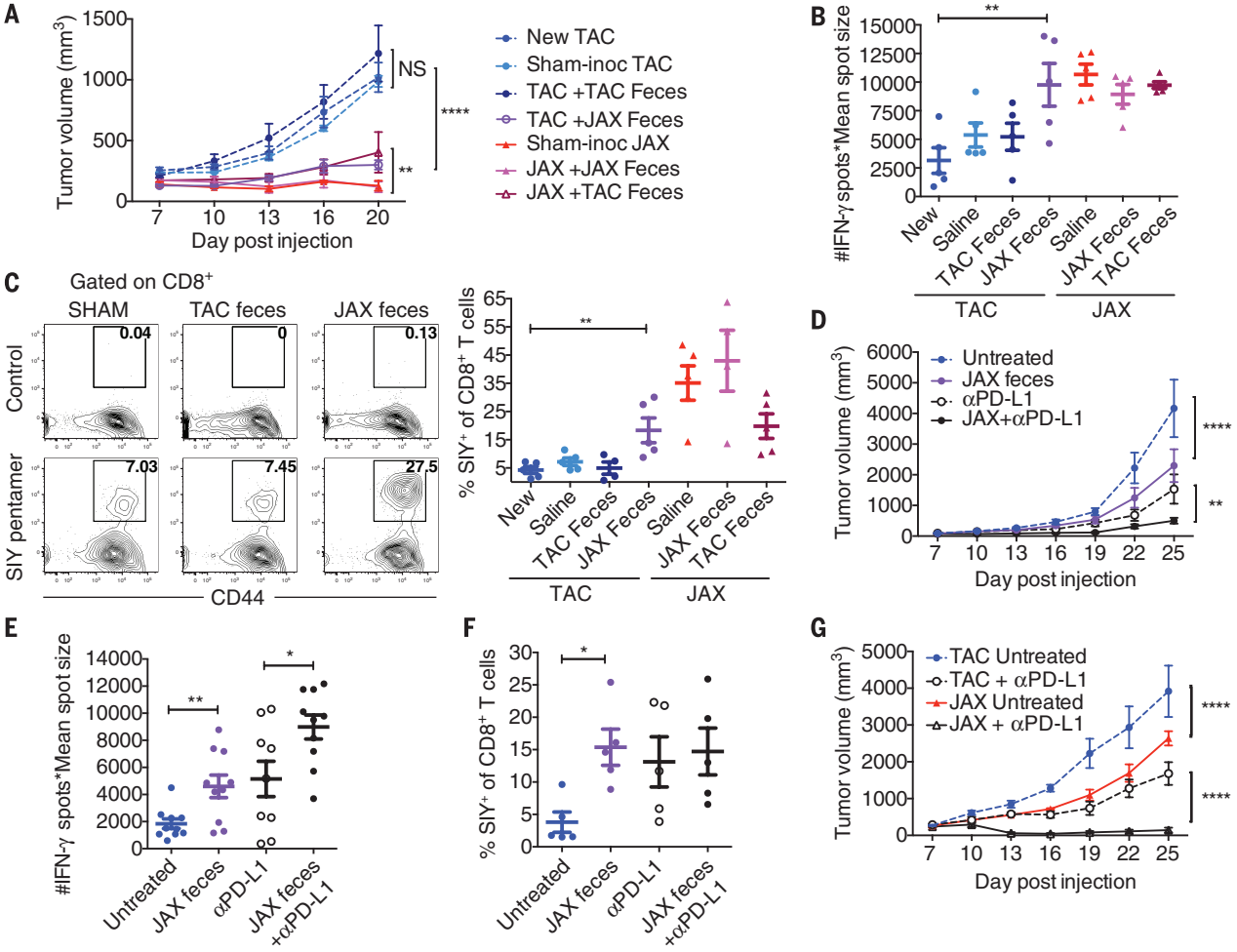

Fig. 2. Oral administration of JAX fecal material to TAC mice enhances spontaneous antitumor immunity and response to αPD-L1 mAb therapy. (**A**) B16.SIY tumor growth in newly arrived TAC mice, TAC and JAX mice orally gavaged with phosphate-buffered saline or TAC or JAX fecal material before tumor implantation. (**B**) Number of IFN-γ spots × mean spot size (10^{-3} mm^2), determined by ELISPOT 7 days after tumor inoculation. (**C**) Percentage of SIY^+ $CD8^+$ T cells within the tumor of TAC and JAX mice treated as in (A), 21 days after tumor inoculation. Representative plots (left), quantification (right). (**D**) B16.SIY tumor growth in TAC mice, untreated or treated with JAX fecal material 7 and 14 days after tumor implantation, αPD-L1 mAb 7, 10, 13, and 16 days after tumor implantation, or both regimens. (**E**) IFN-γ ELISPOT assessed 5 days after start of treatment. (**F**) Percentage of tumor-infiltrating SIY^+ $CD8^+$ T cells, determined by flow cytometry 14 days after start of treatment. (**G**) B16.SIY tumor growth kinetics in TAC and JAX mice, untreated or treated with αPD-L1 mAb 7, 10, 13, and 16 days after tumor implantation. Means ± SEM analyzed by two-way analysis of variance (ANOVA) with Dunnett's (A) or Tukey's (D) and (G) correction for multiple comparisons; or individual mice with means ± SEM analyzed by one-way ANOVA with Holm-Sidak correction for multiple comparisons (B), (C), (E), and (F); data are representative of (A) to (C), (F), and (G) or combined from (D) and (E) two to four independent experiments; five mice per group per experiment; $*P < 0.05$, $**P < 0.01$, $****P < 0.0001$; NS, not significant.

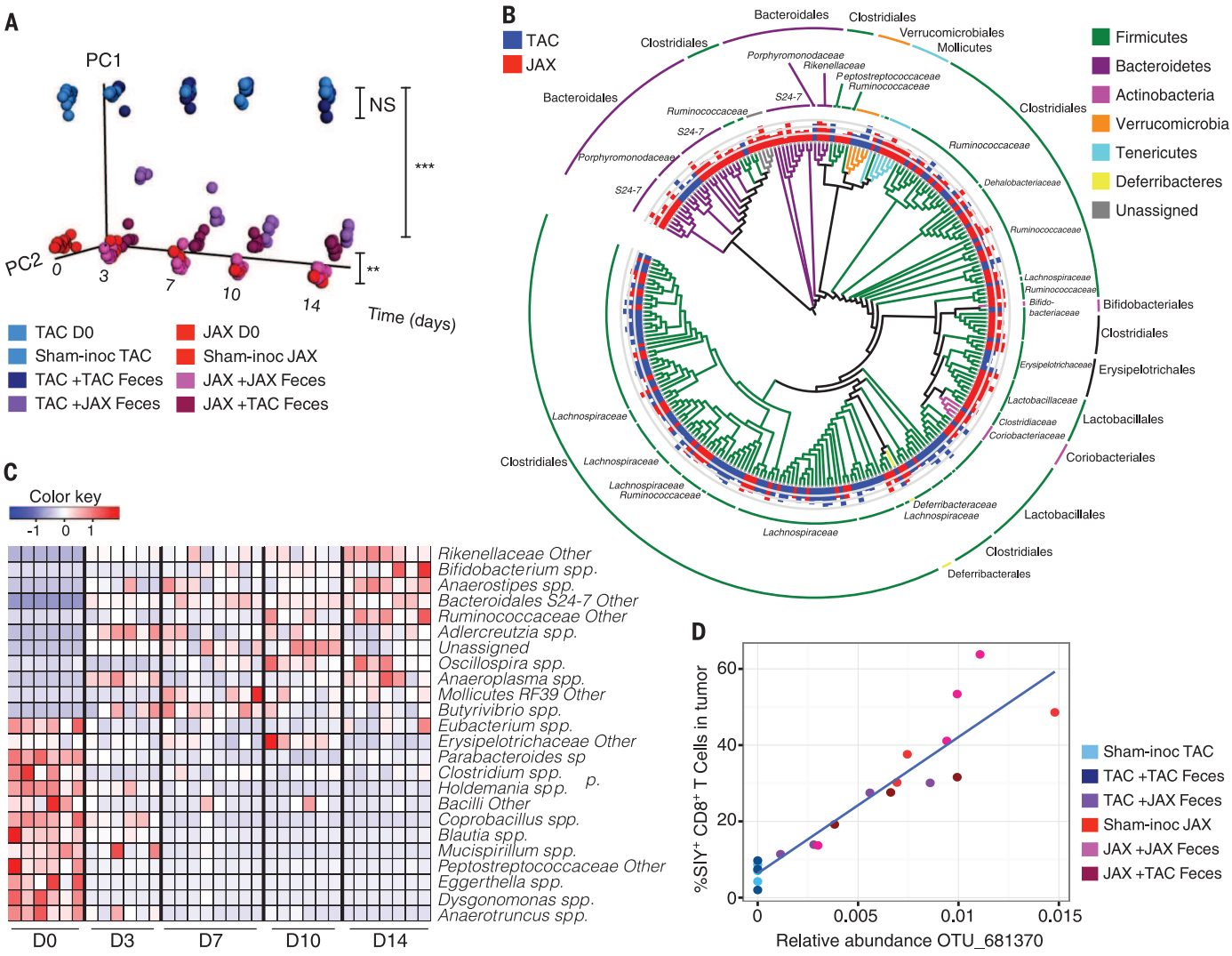

Fig. 3. Direct administration of *Bifidobacterium* to TAC recipients with established tumors improves tumor-specific immunity and response to αPD-L1 mAb therapy. (**A**) Principal coordinate analysis plot of bacterial β-diversity over time in groups treated as in Fig. 2A, each group is made up of at least two cages, three or four mice per cage; data represent three independent experiments; $^{**}P < 0.01$, $^{***}P < 0.001$ (ANOSIM). (**B**) Phylogenetic analysis of taxa that are of significantly different abundance in newly arrived JAX versus TAC mice FDR < 0.05 (nonparametric *t* test); bars represent log-transformed fold changes, inner circle, $\log_{10}(10)$; middle circle, $\log_{10}(100)$; outer circle, $\log_{10}(1000)$. (**C**) Heat map showing relative abundance over time of significantly altered genus-level taxa in JAX-fed TAC mice FDR < 0.05 (nonparametric *t* test); columns depict individual mice; each time point shows mice from two separate cages, three or four mice per cage. (**D**) Correlation plot of relative abundance of *Bifidobacterium* OTU_681370 in fecal material obtained from groups, as in (A), 14 days after arrival and frequency of SIY$^+$ CD8$^+$ T cells in tumor; $P = 1.4 \times 10^{-5}$, FDR = 0.0002, correlation $R^2 = 0.86$ (univariate regression). (**E**) B16.SIY tumor growth kinetics in TAC mice, untreated or treated with *Bifidobacterium* 7 and 14 days after tumor implantation, αPD-L1 mAb 7, 10, 13, and 16 days after tumor implantation, or both regimens. (**F**) IFN-γ ELISPOT assessed 5 days after start of treatment. (**G**) Percentage of tumor-infiltrating SIY$^+$ CD8$^+$ T cells, determined by flow cytometry 14 days after start of treatment. Means ± SEM analyzed by two-way ANOVA with Tukey's correction (E) or individual mice with means ± SEM analyzed by one-way ANOVA with Holm-Sidak correction (F) and (G), and are combined from two independent experiments; five mice per group per experiment: $^{*}P < 0.05$, $^{***}P < 0.001$, $^{****}P < 0.0001$.

isolated from *Bifidobacterium*-gavaged tumor-bearing mice (fig. S5C). We thus concluded that the observed systemic immunological effects are likely occurring independently of bacterial translocation.

We subsequently interrogated the immunologic mechanisms underlying the observed differences in T cell responses between TAC, JAX, and *Bifidobacterium*-treated TAC mice (fig. S6A). $CD8^+$ SIY-specific 2C T cell receptor (TCR) Tg T cells exposed to tumors in JAX and *Bifidobacterium*-treated TAC mice exhibited greater expansion in the tumor-draining lymph node, as compared with their counterparts in TAC mice (fig. S6B). However, they produced markedly greater IFN-γ in both the tumor-draining lymph node and the spleen of JAX and *Bifidobacterium*-fed TAC tumor-bearing mice (Fig. 4A), consistent with our analyses of the endogenous T cell response (Figs. 1C, 2E, and 3F). These data pointed to an improvement in immune responses upstream of T cells, at the level of host dendritic cells (DCs). Consistent with this hypothesis, we found an increased percentage of major histocompatibility complex (MHC) Class II^{hi} DCs in the tumors of JAX and *Bifidobacterium*-treated TAC mice (Fig. 4B).

We therefore used genome-wide transcriptional profiling of early tumor-infiltrating DCs isolated from TAC, JAX, and *Bifidobacterium*-treated TAC mice (fig. S7A and table S5). Pathway analysis of 760 gene transcripts up-regulated in both JAX and *Bifidobacterium*-treated TAC-derived DCs relative to DCs from untreated TAC mice identified cytokine-cytokine receptor interaction, T cell activation, and positive regulation of mononuclear cell proliferation as significantly enriched pathways (Fig. 4C and fig. S7B). Many of these genes have been shown to be critical for antitumor responses, including those involved in $CD8^+$ T cell activation and costimulation [*H2-m2* (MHC-I), *Cd40*, *Cd70*, and *Icam1*] (*20*–*22*); DC maturation (*Relb* and *Ifngr2*) (*23*, *24*); antigen processing and

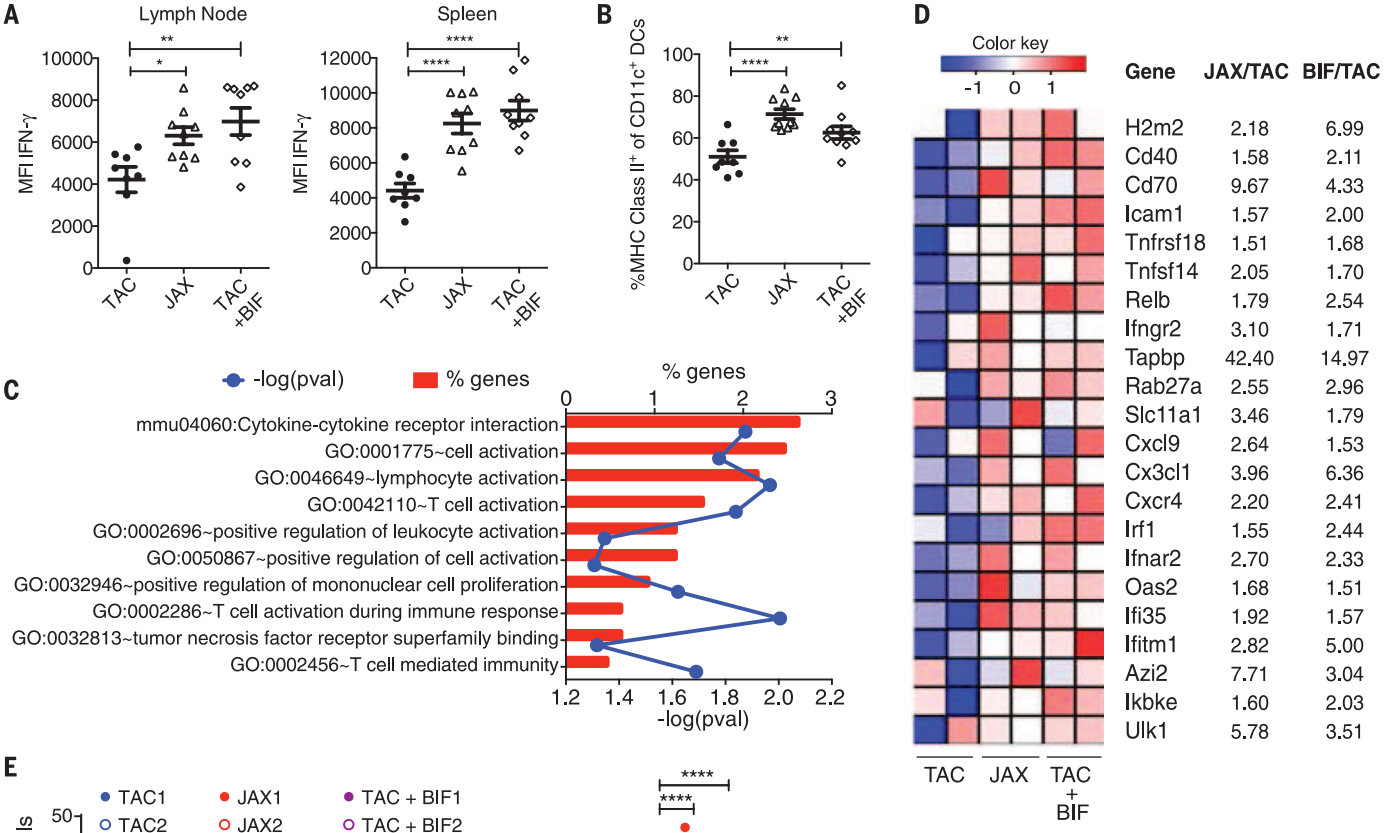

Fig. 4. Dendritic cells isolated from JAX and *Bifidobacterium*-fed TAC mice show increased expression of genes associated with antitumor immunity and heightened capability for T cell activation. (**A**) Quantification of IFN-γ mean fluorescence intensity (MFI) of 2C $CD8^+$ T cells in the tumor-draining lymph node (left) and spleen (right) of TAC, JAX, and *Bifidobacterium*-fed TAC mice on day 7 after adoptive transfer. (**B**) Percentage of MHC Class II^{hi} DCs in tumors isolated from TAC, JAX, and *Bifidobacterium*-fed TAC mice 40 hours after tumor implantation as assessed by flow cytometry. Data in (A) and (B) show individual mice with means ± SEM, analyzed by one-way ANOVA with Holm-Sidak correction; representative of two to four independent experiments, eight or nine mice per group per experiment: $*P < 0.05$, $**P < 0.01$, $****P < 0.0001$. (**C**) Enriched biological pathways and functions found within the subset of elevated genes in JAX and *Bifidobacterium*-treated TAC-derived DCs relative to untreated TAC DCs isolated from tumors 40 hours after tumor inoculation, as assessed by DAVID pathway analysis. Red bars indicate the percentage of genes in a pathway up-regulated in DCs isolated from JAX and *Bifidobacterium*-fed TAC mice. Blue line indicates *P* values calculated by Fisher's exact test. (**D**) Heat map of key antitumor immunity genes in DCs isolated from JAX, *Bifidobacterium*-treated TAC or untreated TAC mice. Mean fold-change for each gene transcript is shown on the right. (**E**) Quantification of IFN-γ^+ 2C TCR Tg $CD8^+$ T cells stimulated in vitro with DCs purified from peripheral lymphoid tissues of naïve TAC, JAX, and *Bifidobacterium*-treated TAC mice in the presence of different concentrations of SIY peptide. Analyses in (C) to (E) were performed on data combined from two independent experiments, five mice pooled per group per experiment. (E) Technical replicates of pooled samples from each experiment separately and were analyzed by fitting a linear mixed model, with Bonferroni correction for multiple comparisons: $*P < 0.05$, $****P < 0.0001$.

cross presentation (*Tapbp*, *Rab27a*, and *Slc11a1*) (*25*–*27*); chemokine-mediated recruitment of immune cells to the tumor microenvironment (*Cxcl9*, *Cx3cl1*, and *Cxcr4*) (*28*–*30*); and type I interferon signaling (*Irf1*, *Ifnar2*, *Oas2*, *Ifi35*, and *Ifitm1*) (*31*, *32*) (Fig. 4D and fig. S7C). Expression of these genes was also increased in murine bone marrow–derived DCs stimulated with *Bifidobacterium* in vitro (table S6), consistent with previous reports that these species of *Bifidobacterium* can directly elicit DC maturation and cytokine production (*13*).

To test whether functional differences in DCs isolated from TAC, JAX, and *Bifidobacterium*-treated TAC mice could be sufficient to explain the differences in T cell priming observed in vivo, we purified DCs from lymphoid tissues of naïve TAC, JAX, and *Bifidobacterium*-treated TAC mice and tested their ability to induce carboxyfluorescein diacetate succinimidyl ester (CFSE)–labeled $CD8^+$ SIY-specific 2C TCR Tg T cell proliferation and acquisition of IFN-γ production in vitro. DCs purified from JAX and *Bifidobacterium*-treated TAC mice induced 2C T cell proliferation at lower antigen concentration than did DCs purified from naïve TAC mice (fig. S8, A and B). Furthermore, at all antigen concentrations, JAX-derived DCs elicited elevated levels of T cell IFN-γ production (Fig. 4E and fig. S8A). We observed similar effects upon oral administration of *Bifidobacterium* to TAC mice before DC isolation (Fig. 4E and fig. S8A). Taken together, these data suggest that commensal *Bifidobacterium*-derived signals modulate the activation of DCs in the steady state, which in turn supports improved effector function of tumor-specific $CD8^+$ T cells.

Our studies demonstrate an unexpected role for commensal *Bifidobacterium* in enhancing antitumor immunity in vivo. Given that beneficial effects are observed in multiple tumor settings and that alteration of innate immune function is observed, this improved antitumor immunity could be occurring in an antigen-independent fashion. The necessity for live bacteria may imply that *Bifidobacterium* colonizes a specific compartment within the gut that enables it to interact with host cells that are critical for modulating DC function or to release soluble factors that disseminate systemically and lead to improved DC function.

Our results do not rule out a contribution of other commensal bacteria species in having the capability to regulate antitumor immunity, either positively or negatively. Our data support the idea that one source of intersubject heterogeneity with regard to spontaneous antitumor immunity and therapeutic effects of antibodies targeting the PD-1/PD-L1 axis may be the composition of gut microbes, which could be manipulated for therapeutic benefit. These principles could apply to other immunotherapies, such as antibodies targeting the CTLA-4 pathway. Similar analyses can be performed in humans, by using 16*S* rRNA sequencing of stool samples from patients receiving checkpoint blockade or other immunotherapies, to identify commensals associated with clinical benefit.

REFERENCES AND NOTES

1. F. S. Hodi *et al.*, *N. Engl. J. Med.* **363**, 711–723 (2010).
2. O. Hamid *et al.*, *N. Engl. J. Med.* **369**, 134–144 (2013).
3. P. C. Tumeh *et al.*, *Nature* **515**, 568–571 (2014).
4. S. Spranger *et al.*, *Sci. Transl. Med.* **5**, 200ra116 (2013).
5. R. R. Ji *et al.*, *Cancer Immunol. Immunother.* **61**, 1019–1031 (2012).
6. T. F. Gajewski, J. Louahed, V. G. Brichard, *Cancer J.* **16**, 399–403 (2010).
7. L. V. Hooper, D. R. Littman, A. J. Macpherson, *Science* **336**, 1268–1273 (2012).
8. I. I. Ivanov II, K. Honda, *Cell Host Microbe* **12**, 496–508 (2012).
9. J. P. McAleer, J. K. Kolls, *Immunity* **37**, 10–12 (2012).
10. N. Iida *et al.*, *Science* **342**, 967–970 (2013).
11. S. Viaud *et al.*, *Science* **342**, 971–976 (2013).
12. I. I. Ivanov II *et al.*, *Cell* **139**, 485–498 (2009).
13. P. López, M. Gueimonde, A. Margolles, A. Suárez, *Int. J. Food Microbiol.* **138**, 157–165 (2010).
14. O. Ménard, M.-J. Butel, V. Gaboriau-Routhiau, A.-J. Waligora-Dupriet, *Appl. Environ. Microbiol.* **74**, 660–666 (2008).
15. P. Dong, Y. Yang, W. P. Wang, *Early Hum. Dev.* **86**, 51–58 (2010).
16. T. Kawahara *et al.*, *Microbiol. Immunol.* **59**, 1–12 (2015).
17. N. Arpaia *et al.*, *Nature* **504**, 451–455 (2013).
18. P. M. Smith *et al.*, *Science* **341**, 569–573 (2013).
19. K. Atarashi *et al.*, *Science* **331**, 337–341 (2011).
20. M. F. Mackey *et al.*, *J. Immunol.* **161**, 2094–2098 (1998).
21. A. Scholer, S. Hugues, A. Boissonnas, L. Fetler, S. Amigorena, *Immunity* **28**, 258–270 (2008).
22. S. P. Bak *et al.*, *J. Immunol.* **189**, 1708–1716 (2012).
23. J. Pan *et al.*, *Immunol. Lett.* **94**, 141–151 (2004).
24. A. R. Pettit *et al.*, *J. Immunol.* **159**, 3681–3691 (1997).
25. E. B. Compeer, T. W. H. Flinsenberg, S. G. van der Grein, M. Boes, *Front. Immunol.* **3**, 37 (2012).
26. C. Jancic *et al.*, *Nat. Cell Biol.* **9**, 367–378 (2007).
27. C. B. Stober, S. Brode, J. K. White, J. F. Popoff, J. M. Blackwell, *Infect. Immun.* **75**, 5059–5067 (2007).
28. K. Kabashima *et al.*, *Am. J. Pathol.* **171**, 1249–1257 (2007).
29. M. Nukiwa *et al.*, *Eur. J. Immunol.* **36**, 1019–1027 (2006).
30. L. Zhang *et al.*, *N. Engl. J. Med.* **348**, 203–213 (2003).
31. M. B. Fuertes *et al.*, *J. Exp. Med.* **208**, 2005–2016 (2011).
32. S.-R. Woo *et al.*, *Immunity* **41**, 830–842 (2014).

ACKNOWLEDGMENTS

R code for gene expression analyses can be found at https://github.com/kipkeston/TG_Microbiota; microarray data can be found at www.ncbi.nlm.nih.gov/geo/query/acc.cgi?acc=GSE73475 and www.ncbi.nlm.nih.gov/geo/query/acc.cgi?acc=GSE73476; 16*S* rRNA sequencing data can be found at www.ncbi.nlm.nih.gov/bioproject/297465. The data reported in this manuscript are presented in the main paper and in the supplementary materials. We thank D. Ringus for anaerobic culture of bifidobacteria and colony quantification, Y. Zhang for providing *Lactobacillus murinus* cultures, and R. Sweis for providing the MB49 bladder cancer cell line. This work was supported by a Team Science Award from the Melanoma Research Alliance, and National Institute of Diabetes and Digestive and Kidney Diseases, NIH, P30 Digestive Disease Research Core Center Grant (DK42086), the University of Chicago Cancer Biology training program (5T32CA009594-25), and the Cancer Research Institute fellowship program. The University of Chicago has filed a patent application that relates to microbial community manipulation in cancer therapy.

SUPPLEMENTARY MATERIALS

www.sciencemag.org/content/350/6264/1084/suppl/DC1
Materials and Methods
Figs. S1 to S8
Tables S1 to S7
References (*33*–*42*)

25 April 2015; accepted 9 October 2015
Published online 5 November 2015
10.1126/science.aac4255

MALARIA

Malaria parasites target the hepatocyte receptor EphA2 for successful host infection

Alexis Kaushansky,[1]* Alyse N. Douglass,[1] Nadia Arang,[1] Vladimir Vigdorovich,[1] Nicholas Dambrauskas,[1] Heather S. Kain,[1] Laura S. Austin,[1,2] D. Noah Sather,[1] Stefan H.I. Kappe[1,2]*

The invasion of a suitable host hepatocyte by mosquito-transmitted *Plasmodium* sporozoites is an essential early step in successful malaria parasite infection. Yet precisely how sporozoites target their host cell and facilitate productive infection remains largely unknown. We found that the hepatocyte EphA2 receptor was critical for establishing a permissive intracellular replication compartment, the parasitophorous vacuole. Sporozoites productively infected hepatocytes with high EphA2 expression, and the deletion of EphA2 protected mice from liver infection. Lack of host EphA2 phenocopied the lack of the sporozoite proteins P52 and P36. Our data suggest that P36 engages EphA2, which is likely to be a key step in establishing the permissive replication compartment.

Malaria infections place a tremendous burden on global health (*1*). Their causative agents, *Plasmodium* parasites, are transmitted to mammals as sporozoites by the bite of *Anopheles* mosquitoes. After entry into a capillary, sporozoites are carried to the liver, where they pass through multiple cells before recognizing and invading hepatocytes. During invasion, the sporozoite forms a protective parasitophorous vacuole made of hepatocyte plasma membrane, which ensconces the parasite, establishes the intrahepatocytic replication

[1]Center for Infectious Disease Research (formerly Seattle Biomedical Research Institute), 307 Westlake Avenue North, No. 500, Seattle, WA 98109, USA. [2]Department of Global Health, University of Washington, Seattle, WA 98195, USA. ***Corresponding author. E-mail: alexis.kaushansky@cidresearch.org (A.K.); stefan.kappe@cidresearch.org (S.H.I.K.)**

Commensal *Bifidobacterium* promotes antitumor immunity and facilitates anti–PD-L1 efficacy

Ayelet Sivan, Leticia Corrales, Nathaniel Hubert, Jason B. Williams, Keston Aquino-Michaels, Zachary M. Earley, Franco W. Benyamin, Yuk Man Lei, Bana Jabri, Maria-Luisa Alegre, Eugene B. Chang and Thomas F. Gajewski (November 5, 2015)

Science **350** (6264), 1084-1089. [doi: 10.1126/science.aac4255] originally published online November 5, 2015

Editor's Summary

Gut microbes affect immunotherapy

The unleashing of antitumor T cell responses has ushered in a new era of cancer treatment. Although these therapies can cause dramatic tumor regressions in some patients, many patients inexplicably see no benefit. Mice have been used in two studies to investigate what might be happening. Specific members of the gut microbiota influence the efficacy of this type of immunotherapy (see the Perspective by Snyder *et al.*). Vétizou *et al.* found that optimal responses to anticytotoxic T lymphocyte antigen blockade required specific *Bacteroides* spp. Similarly, Sivan *et al.* discovered that *Bifidobacterium* spp. enhanced the efficacy of antiprogrammed cell death ligand 1 therapy.

Science, this issue, p. 1079 and p. 1084; see also p. 1031

Università Vita-Salute San Raffaele

Prova di selezione per l'ammissione al corso di Laurea Magistrale in BIOTECNOLOGIE MEDICHE MOLECOLARI E CELLULARI
3 Ottobre 2016

Titolo (0-10 punti)

Abstract (0-10 punti)

Università Vita-Salute San Raffaele

Prova di selezione per l'ammissione al corso di Laurea Magistrale in BIOTECNOLOGIE MEDICHE MOLECOLARI E CELLULARI
3 Ottobre 2016

DOMANDE A RISPOSTA LIBERA
(0-9 punti/domanda)

1. Come è dimostrato in questo studio il ruolo del microbioma nel modulare l'immunità anti-tumorale?

2. Nello studio la secrezione di IFN-gamma è utilizzata per monitorare le risposte cellulari T antigene-specifiche. Perchè è stata scelta questo molecola e quali altre citochine avrebbero potuto essere utilizzate per caratterizzare una risposta T citotossica?

Università Vita-Salute San Raffaele

Prova di selezione per l'ammissione al corso di Laurea Magistrale in BIOTECNOLOGIE MEDICHE MOLECOLARI E CELLULARI
3 Ottobre 2016

DOMANDE A RISPOSTA MULTIPLA
(risposta esatta: +2 –risposta omessa: 0 - risposta errata o invalidata: -0.75 –)

1. *Quali caratteristiche accomunano o differenziano i topi C57BL/6 allevati presso il Jackson Laboratory (JAX) e la Taconic Farm (TAC)?*

A. I topi dei due centri possiedono un differente background genetico ❑
B. I topi dei due centri possiedono un differente microbioma ❑
C. La crescita del tumore B17.SIY ha una cinetica analoga nei topi dei due centri ❑
D. Tutte le precedenti risposte sono corrette ❑

2. *I tumori B17.SIY che crescono nei topi JAX*

A. Sono maggiormente infiltrati da linfociti T $CD8^+$ ❑
B. Sono maggiormente infiltrati da linfociti T tumore-specifici ❑
C. Tutte le precedenti risposte sono corrette ❑
D. Sono maggiormente infiltrati da linfociti T $CD4^+$ ❑

3. *Il trasferimento profilattico di materiale fecale da topi TAC in topi JAX rispetto al trasferimento di materiale fecale da topi JAX in topi JAX…*

A. Accelera significativamente la crescita del tumore B17.SIY ❑
B. Rallenta significativamente la crescita del tumore B17.SIY ❑
C. Non modifica in modo significativo la crescita del tumore B17.SIY ❑
D. Nessuna risposta è corretta ❑

4. *Il trasferimento profilattico di materiale fecale da topi JAX in topi TAC e la somministrazione di anticorpi anti-PD-L1…*

A. Incrementa significativamente la % di linfociti T $CD8^+$ specifici per SIY nel tumore rispetto ai topi trattati con solo anti-PD-L1 ❑
B. Incrementa significativamente la % di linfociti T $CD8^+$ specifici per SIY nel tumore rispetto ai topi trattati con solo materiale fecale ❑
C. Non incrementa significativamente la % di linfociti T CD8+ specifici per SIY nel tumore rispetto ai topi non trattati ❑
D. Nessuna risposta è corretta ❑

5. *Il microbiota dei topi TAC trattati con materiale fecale da JAX…*

A. Si arricchisce di *Egghertheliа spp* ❑
B. Si depaupera di *Bifidoacterium spp* ❑
C. Si arricchisce di *Bifidoacterium spp* ❑
D. Nessuna risposta è corretta ❑

6. La somministrazione di Bifidoacterium *e di anticorpi anti-PD-L1…*
A. Ha un effetto analogo sulla crescita del tumore B16.SIY ❑
B. Ha un effetto analogo sull'incremento di linfociti T $CD8^+$ specifici per SIY nel tumore ❑
C. Ha un effetto più curativo se i topi subiscono entrambi i trattamenti ❑
D. Tutte le risposte sono corrette ❑

7. I batteri somministrati a topi TAC inducono rallentamento nella crescita del tumore B16.SIY…
A. Questa affermazione è vera nel caso di *Bifidoacterium* ❑
B. Questa affermazione è sempre vera ❑
C. Questa affermazione è vera solo nel caso del *Lactobacillus murinus* ❑
D. Questa affermazione è sempre falsa ❑

8. L'effetto antitumorale della somministrazione di Bifidoacterium…
A. Dipende dalla traslocazione batterica nei linfonodi ❑
B. Dipende dalla traslocazione batterica nel tumore ❑
C. E' indipendente dalla traslocazione batterica nei linfonodi, nella milza e nel tumore ❑
D. Dipende dalla traslocazione batterica nella milza ❑

9. *Ad una settimana dal loro trasferimento adottivo, cellule T $CD8^+$ specifiche per SIY producono più IFN-gamma…*
A. Nel linfonodo e milza dei topi TAC rispetto agli altri gruppi sperimentali ❑
B. Nella sola milza dei topi TAC rispetto agli altri gruppi sperimentali ❑
C. Negli organi esaminati dai topi JAX rispetto ai topi TAC ❑
D. Nel linfonodo e milza dei topi JAX rispetto agli altri gruppi sperimentali ❑

10. Cellule dendritiche ad alta espressione di MHC di classe II sono riscontrate in maggiore percentuale…
A. Nei linfonodi drenanti il tumore dei topi TAC rispetto ai topi JAX ❑
B. Nelle milze drenanti dei topi JAX rispetto ai topi TAC trattati con *Bifidobacterium* ❑
C. Nei tumori dei topi JAX rispetto ai topi TAC ❑
D. Nessuna risposta è corretta ❑

11. Nella Figura 1, pannello C, si utilizza il "mean size" degli spot di IFN-gamma, questo parametro riflette…
A. Il numero di cellule per piastra che producono citochina ❑
B. Il numero di cellule per spot che producono la citochina ❑
C. La quantità di citochina prodotta da ciascun clone cellulare ❑
D. La quantità di citochina prodotta da ciascuna cellula ❑

12. La Figura 1, pannello D, mostra una maggiore frequenza di cellule positive per la colorazione con pentameri XY nei topi JAX rispetto ai topi TAC. Questa colorazione identifica i linfociti che esprimono…

A. IFN-g□□□□ ❑
B. CD8 ❑
C. HMC-specifici per uno specifico peptide ❑
D. TCR specifici per uno specifico peptide ❑

13. Commentando la Figura 2, gli autori descrivono un "JAX-dominant effect". Tale effetto presuppone che…

A. Le feci dei topi JAX siano popolate da un microbioma in grado di colonizzare più velocemente ed efficacemente rispetto a quelle di topi TAC ❑
B. Le feci dei topi TAC siano popolate da un microbioma in grado di colonizzare più velocemente ed efficacemente rispetto a quelle di topi JAX ❑
C. Il microbioma dei topi TAC trasferito nei topi JAX sia incapace di influire immunologicamnete sul microbioma dei topi JAX ❑
D. Il microbioma dei topi JAX trasferito nei topi TAC sia incapace di influire immunologicamente sul microbioma dei topi TAC ❑

14. Nella Figura 2, pannello F, la percentuale di linfociti positive alla colorazione con pentamero risulta simile dopo il trapianto di feci dai topi JAX in topi trattati con anticorpi anti-PDL1 e con la combinazione di questi due trattamenti. Questo risultato suggerisce che i due trattamenti agiscano…

A. Sullo stesso target ❑
B. Su target differenti ❑
C. In sinergia ❑
D. In antagonismo ❑

15. L'efficacia degli anticorpi anti-PDL1 in questo sistema presuppone che…

A. Il microbioma influenzi la capacità dei linfociti di essere eliminati per morte cellulare programmata ❑
B. Gli anticorpi abbiano la capacità d'interferire con linfociti T-regolatori in grado di bloccare la risposta anti-tumore ❑
C. L'esistenza di una risposta anti-tumorale mediata da linfociti T ❑
D. L'esistenza di una risposta T cellulare specifica per antigeni del microbioma ❑

16. Nello studio, la scelta del Bifidoacterium *come agente per il trattamento dei topi TAC è basata sulla seguente premessa:*

A. Le feci dei topi JAX contengono molto meno *Bifidoacterium* ❑
B. La presenza del *Bifidoacterium* è associata positivamente alla comparsa di T cellule ad azione anti-tumorale ❑
C. La presenza del *Bifidoacterium rium* è associata negativamente alla comparsa di T cellule ad azione anti-tumorale ❑
D. Il *Bifidoacterium* è uno dei costituenti fondamentali delle preparazioni commerciali utilizzata dall'industria casearia ❑

17. Il trattamento con il Bifidoacterium *si è dimostrato in grado di:*

A. Aumentare in modo significativo il numero di linfociti specifici infiltranti il tumore, ma non quelli presenti in periferia ❑
B. Aumentare in modo significativo il numero di linfociti specifici presenti in periferia, ma non quelli infiltranti il tumore ❑
C. Aumentare in modo significativo il numero di linfociti specifici infiltranti il tumore e presenti in periferia ❑
D. Aumentare in modo significativo il numero di linfociti specifici infiltranti il tumore, ma solo in combinazione con anticorpi anti-PDL1 ❑

18. L'alta espressione di antigeni MHC di Classe II sulle cellule dendritiche CD11c$^+$ viene utilizzata nel pannello B della Figura 4 per indicare…

A. La capacità migratoria delle cellule all'interno del tumore ❑
B. Lo stato di maturazione delle cellule ❑
C. La capacità di sopravvivere alla morte cellulare indotta da *cross-linking* di molecule MHC ❑
D. La capacità di produrre IFN-gamma ❑

19. Secondo gli autori gli effetti sull'espressione genica di cellule dendritiche in animali trattati con Bifidoacterium *potrebbero essere conseguenza della capacità dei batteri di…*

A. Attivare linfociti a livello della mucosa intestinale ❑
B. Essere trasportati nei linfonodi drenanti ❑
A. Interagire direttamente con le cellule dendritiche ❑
B. Interagire direttamente con i linfociti T CD8$^+$ ❑

20. La proliferazione delle cellule T marcate con il fluorocromo CSFE è valutata mediante citometria a flusso…

A. Monitorando la quantità di colorante che interagisce effettivamente con la cromatina decondensata ❑
B. Valutando la capacità del colorante di associarsi a Ki67 ❑
C. Valutando la capacità del colorante di associarsi alle proteine di nuova sintesi durante la duplicazione cellulare ❑
D. Valutando la diluizione del colorante in modo proporzionale ai cicli di proliferazione cellulare ❑

21. La risposta dei pazienti all'immunoterapia discussa nell'articolo è migliore se...

A. Nei pazienti è già presente una risposta T cellulare ❑
B. Nei pazienti è già presente una risposta B cellulare ❑
C. Nei pazienti è già presente una risposta immunitaria innata ❑
D. Nessuna risposta è corretta ❑

22. La coabitazione dei due ceppi di topi utilizzati nello studio ha comportato…

A. Nessun particolare effetto sulla crescita tumorale nei due ceppi di topo ❑
B. Una modificazione della risposta immunitaria nei due ceppi di topo, senza influenzare la crescita tumorale ❑
C. Una modificazione della crescita tumorale senza influenzare la risposta immunitaria nei due ceppi di topo ❑
D. L'abolizione delle differenze sia di crescita tumorale che di risposta immunitaria nei due ceppi murini ❑

23. L'efficacia della terapia con Ab anti-PD-L1 è…

A. Simile nei due ceppi di topo ❑
B. Superiore nei topi JAX ❑
C. Superiore nei topi TAC ❑
D. Nessuna risposta è corretta ❑

24. la caratterizzazione del microbiota dei due ceppi di topi è stata condotta mediante…

A. Semina in soft Agar e crescita delle colonie batteriche ❑
B. Amplificazione selettiva di note regioni di genoma batterico recante mutazioni di resistenza agli antibiotici ❑
C. Mediante amplificazione del DNA batterico ❑
D. Mediante sequenziamento dell'RNA ribosomiale 16S ❑

25. Un'analisi statistica dello studio ha utilizzato il "False Discovery Rate (FDR)" che potrebbe essere definito come…

A. Un metodo che identifica la presenza di dati falsi nello studio ❑
B. E' un metodo utilizzato per valutare confronti multipli con misure ripetute ❑
C. E' sinonimo del metodo di Bonferroni ❑
D. Nessuna risposta è corretta ❑

26. Nello studio è utilizzato il colorante CSE; quali altri metodi avrebbero potuto essere impiegati per ottenere la stessa informazione?

A. Incorporazione di timidina triziata ❑
B. Rilascio di Perforina ❑
C. Secrezione di IL-2 ❑
D. Espressione di fosfatidil-serina sulla superficie cellulare ❑

27. Un'importante condizione controllo dello studio è stata …

A. L'indagine del possibile effetto di *Bifidobacterium* sulla risposta immunitaria in animali non portatori di tumori ❑
B. Utilizzare un'infezione virale e non batterica come controllo di specificità ❑
C. Inoculare i topi TAC con *Bifidobacterium* inattivato al calore ❑
D. Nessuna risposta è corretta ❑

28. Nello studio, l'effetto del Bifidobacterium nei topi TAC è abolito da…

A. Eliminazione di linfociti T $CD4^+$ ❑
B. Eliminazione dei linfociti B ❑
C. Eliminazione di linfociti T $CD8^+$ ❑
D. Neutralizzazione dell'IFN-gamma ❑

29. Altri batteri simili al Bifidobacterium (B. breve e B. longum) *hanno causato effetti…*

A. Simili al *Bifidobacterium* ❑
B. Aumentati rispetto al *Bifidobacterium* ❑
C. Irrilevanti rispetto alla crescita tumorale ❑
D. D'immunosopressione nell'animale ospite ❑

30. Le cellule T regolatorie, in questo studio, hanno dimostrato…

A. Di giocare un ruolo fondamentale nella risposta a variazioni del Microbiota rispetto al controllo del tumore ❑
B. Di non giocare un ruolo fondamentale nella risposta a variazioni del microbiota rispetto al controllo del tumore ❑
C. Di modulare la risposta $CD8^+$, fondamentale per il controllo del tumore ❑
D. Nessuna risposta è corretta ❑